Anomalous neutron Compton scattering: Comparison of the convolution approximation with a model-free approach

M. Krzystyniak* and C. A. Chatzidimitriou-Dreismann
Institute of Chemistry, Stranski Laboratory, Technical University Berlin, D-10623 Berlin, Germany
(Received 3 August 2005; revised manuscript received 2 September 2005; published 30 November 2005)

A shortfall of the scattering intensity from protons has been observed in liquids (water, benzene, etc.) and solids (metal hydrogen systems, organic polymers, etc.) using neutron Compton scattering (NCS). However, the suitability of the conventional NCS data reduction scheme, used to obtain the scattering intensities, based on the convolution approximation (CA) of the nuclear momentum distribution with the instrument resolution function has been questioned. In the present work the commonly used data reduction scheme is compared to a model-free approach [B. Dorner, J. Neutron Res. (to be published)] that is independent of the form of the momentum distribution and the resolution function. Specifically, the ratios of the scattering cross section density of H to C are presented for polyethylene. The model-free approach is shown to lead to the same results as for experimental data published earlier and treated with the CA thus addressing a great part of the previous comments.

DOI: 10.1103/PhysRevB.72.174117 PACS number(s): 61.12.Ex, 03.65.Yz, 03.65.Nk, 34.90.+q

I. INTRODUCTION

During the past decade a striking phenomenon of anomalous scattering intensity of epithermal neutrons from hydrogen has been measured in various materials[1–6] using the neutron Compton scattering (NCS) technique. Until very recently the effect has been measured on a unique instrument—i.e., on the time-of-flight spectrometer VESUVIO (formerly eVS) at the ISIS neutron spallation source at the Rutherford Appleton Laboratory, UK. An independent experimental confirmation of the effect has been achieved (in a solid polymer) using a different experimental method—i.e., electron-proton Compton scattering.[7] These experiments have attracted major interest by the international scientific community.[8–10]

VESUVIO is an "inverse-geometry" time-of-flight spectrometer (see Sec. II). The final neutron energy after scattering from a sample is analyzed using a filter with resonant neutron absorption properties (e.g., gold or uranium). The usually applied data reduction scheme is based on the so-called "convolution approximation" (see Sec. II). In the framework of the convolution approximation (CA) it is assumed that the final energy resolution function is well described by a Voigt function centered at the resonance absorption energy of the analyzer foil.[11] A time-of-flight spectrum is described by a convolution of the total resolution function of the instrument, including the final energy resolution function, and the neutron Compton profile of the scatterer[11] (see Sec. II).

However, it has been claimed that the NCS data reduction scheme based on the CA contains various artifacts that are responsible for the striking experimental results.

Blostein *et al.*[12–14] introduced an alternative to the CA data reduction scheme (hereinafter called the "exact formalism") to describe a time-of-flight spectrum in an inverse-geometry spectrometer. The energy resolution function, according to Blostein *et al.*,[12–14] should be described by a total absorption cross-section curve at all final energies of neutrons after scattering from a sample. For example, for gold foil, used commonly at the VESUVIO spectrometer as final energy analyzer,[11] such a total absorption curve[15] would include the $1/\sqrt{E}$ contribution at small final energies, followed by a sharp resonance at a final energy of 4.9 eV and additional smaller resonances at higher energies. In the exact formalism the count rate at a given time of flight is calculated as an integral over the whole range of initial neutron energies.[12,13] Alternatively, after a variable change in the integral taking into account the kinematic relation between initial and final neutron energy at a fixed time-of-flight value, the integral can be calculated over the whole range of final neutron energies.[14] Thus, in this approach the count rate cannot be reduced to a single convolution of the resolution function with the neutron Compton profile.[12–14]

The importance of the assessment of the inaccuracies introduced by the CA was discussed by Chatzidimitriou-Dreismann *et al.*[1] in a published measurement of cross-section anomalies in H_2O-D_2O mixtures. Blostein *et al.*,[12] commenting on this work claimed the existence of errors in the determined areas of overlapping recoil peaks; this was addressed with an experimental test by Chatzidimitriou-Dreismann *et al.*[16] The authors analyzed in particular the case of the considerable overlapping of the strong proton peak with the weak deuteron peak. The experimental test consisted in comparing the deuteron peak areas determined from NCS data of H/D mixed systems, taken in both the forward- and backward-scattering directions. The experimental results from pure D_2O and the equimolar H_2O-D_2O mixture were presented. For both systems, it was shown that the deuteron peak areas in the forward- and backward-scattering directions were essentially equal. Thus, it was concluded that the aforementioned comment appeared not to be of relevance in this specific context.

Motivated by the comments of Blostein *et al.*,[12,13] Mayers and Abdul-Redah[11] showed that it is more convenient to use the CA to analyze NCS data collected on an inverse-geometry (see Sec. II) instrument such as VESUVIO. The

authors[11] discussed in detail the validity of the expressions for the count rate in the time-of-flight domain, the applicability of the impulse approximation, the inclusion of the resolution function as a single convolution in the time of flight, the assumption of the Gaussian form of the nuclear momentum distribution, and finally, multiple scattering and sample attenuation effects in the neutron Compton studies under consideration. They also measured different H_2O-D_2O mixtures[11] with a uranium foil analyzer and compared with previously published data[1] taken with the gold analyzer. The magnitude of the observed anomaly of the scattering cross section from protons was much larger than the systematic errors introduced by the CA for both Au and U filters. Simulations of measurements on other systems also indicated that in all cases the systematic errors of the CA are small and do not significantly affect the results obtained.[11]

A further experimental check on the possible systematic errors introduced by the CA was performed using the double-difference technique.[17] This technique leads to the removal of the long wings of the energy resolution function whatever their functional form. Mayers and Abdul-Redah showed that anomalies of the scattering intensity from protons of the equimolar H_2O-D_2O mixture and a solid polymer[11] and different H_2O-D_2O mixtures[18] obtained using the conventional single-difference and the double-difference techniques were essentially the same.

Moreover, the results reported above were recently confirmed using an independent technique—i.e., electron-proton Compton scattering.[7] In this method, a spectrometer is used with continuous electron beam, where the energy resolution function is a Gaussian and does not contain any long tails and no "foil-in–foil-out" difference is applied.

Very recently, Senesi *et al.*[19] performed and analyzed NCS measurements from orthorombic-ordered HCl using both the exact formalism[12–14,20] and the CA. In the exact formalism the total absorption cross-section curve for gold in the entire energy range[15] was incorporated into the data analysis as the energy resolution function. The results of the analysis using both data reduction schemes were compared. Results of the exact formalism show a 34% reduction of the H cross-section density, varying with the scattering angle in a range centered at 53° (Ref. 19). The magnitude of the anomaly as determined by the exact formalism and the CA was shown to agree at least within an accuracy level of 5%–6%. The authors conclude that this result proves the essential reliability of all previous work done on the anomalous NCS proton cross sections.[19]

Other comments by Cowley[21] were based on the claim that in the NCS data reduction procedure using the CA, as applied on VESUVIO, two factors needed for a direct comparison of the scattering intensities with the tabulated values are not accounted for. The first is the variation of the incident neutron flux with the incident neutron energy. The second factor is the Jacobian of the transformation of the time-of-flight data from a constant scattering angle scan, as recorded at VESUVIO, into a constant momentum transfer scan. These comments were discussed and clarified in an instrumental paper about the VESUVIO spectrometer by Mayers and Abdul-Redah.[11]

The objective of this paper is to present a model-free approach proposed by Dorner[22] and to compare it with the commonly used data reduction scheme based on the CA. Dorner's scheme is independent of the momentum distribution of the target atoms and of the mass-dependent resolution function of the instrument. It is also shown that Dorner's scheme includes all corrections proposed by Cowley[21] mentioned above. The results obtained using the NCS data reduction scheme proposed by Dorner confirm the previously published results obtained using the CA approach, i.e., we show that the anomalies of the scattering intensities from protons are independent of the form of the instrument resolution function, the momentum distribution of the target nuclei, the inclusion of Cowley's Jacobian factor, and the normalization with incident neutron flux.

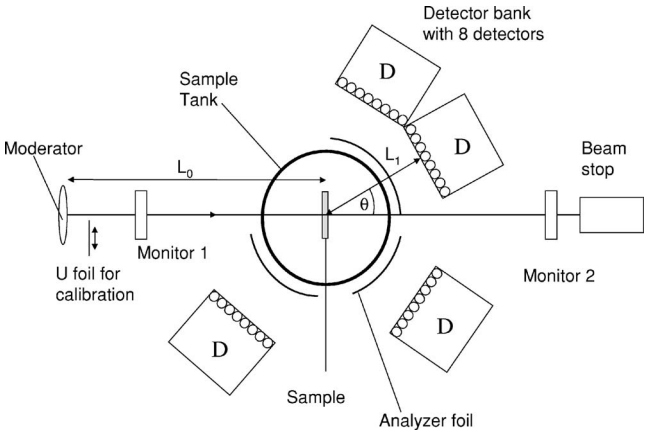

FIG. 1. A schematic representation of the VESUVIO spectrometer at ISIS.

The structure of the paper is the following. We briefly describe the instrument. We continue with the detailed description of the conventional NCS data analysis procedure. Then we present the data reduction scheme proposed by Dorner and compare the results of both data treatments for data collected on a polyethylene sample.

II. CONVOLUTION APPROXIMATION AT VESUVIO

The VESUVIO spectrometer is an inverted-geometry time-of-flight instrument.[11] Incident neutrons travel a distance L_0 from the pulsed source to the sample. After scattering at an angle θ, neutrons of final energy E_1 travel a distance L_1 to the detector position (Fig. 1).

The sample is exposed to a polychromatic neutron beam. The energy E_1 of the neutron after the scattering process is analyzed by taking two spectra, one with a thin foil of a neutron absorbing material between the sample and the detector and one without such a foil. The spectrum to be analyzed is obtained by taking the difference of these two spectra. This standard technique is referred to as the single-difference (SD) technique.

In all NCS experiments on VESUVIO the accessible quantity is the double-differential cross section $d^2\sigma/[d\Omega dE_1]$. Following van Hove's scattering formalism,[23,24] the double-differential cross section is related to the dynamic structure factor $S(\mathbf{q},\omega)$. In what follows $S(\omega,\mathbf{q})$ is assumed to depend only on the magnitude of the

momentum transfer $q=|\mathbf{q}|$ (for a more general approach, see the Appendix). This is the case for all studies concerning neutron Compton scattering where the striking anomaly of the scattering intensity from protons was found (see, e.g., Refs. 1–6). For one type of scattering atoms one can write

$$\frac{d^2\sigma}{d\Omega dE_1} = Nb^2\sqrt{\frac{E_1}{E_0}}S(q,\omega). \tag{1}$$

Here b is the bound scattering length, $d\Omega$ the solid angle and dE_1 the range of final energies into which the neutron is scattered, N is the particle number density, E_0 and E_1 are the initial and final neutron energies, respectively, and q and ω are the transferred momentum and energy, respectively.

The double-differential cross section $d^2\sigma/[d\Omega dE_1]$ is calculated per unit incident flux into a solid angle $d\Omega$ and an energy interval dE_1 (Ref. 24). The incident neutron flux varies with incident neutron energy E_0 and has a distribution $I(E_0)dE_0$ (Ref. 21). The count rate $C(E_0)$ in an NCS experiment is then proportional to $\sqrt{[E_1/E_0]}I(E_0)S(q,\omega)$ (Ref. 21).

In the inverse-geometry spectrometer each detector has a constant angular acceptance $\Delta\Omega$ for any energy and the E_1 energy resolution is fixed by the resonance width of the absorbing foil.[11,21] Also the detector efficiency $D(E_1)$ is fixed. Thus, the count rate $C(E_0)$ measured in a detector placed at given scattering angle θ is given by

$$C(\theta=\text{const},E_0) = Nb^2\sqrt{\frac{E_1}{E_0}}I(E_0)\Delta\Omega D(E_1)S(q,\omega). \tag{2}$$

The spectra are, however, recorded and plotted as a function of time of flight instead of E_0, so $C(t)=C(E_0)dE_0/dt$ (Ref. 21). The Jacobian dE_0/dt is well known in the NCS literature[11]:

$$\frac{dE_0}{dt} = \frac{2}{L_0}\sqrt{\frac{2}{m}}E_0^{3/2}. \tag{3}$$

Using the Jacobian dE_0/dt one can easily derive the expression for the count rate $C(\theta=\text{const},t_i)$:

$$C(\theta=\text{const},t_i) = Nb^2\frac{2}{L_0}\sqrt{\frac{2E_1}{m}}\Delta\Omega D(E_1)E_0(t_i)I(E_0(t_i))S(q(t_i),\omega(t_i)). \tag{4}$$

The energy and momentum transfers from the neutron to the scattering nuclei are so high that the scattering process can be treated within the impulse approximation (IA) limit.[25–30] In the IA limit—i.e., infinite q—$S(q,\omega)$ reduces to a single peak centered at the recoil energy $\omega_r=q^2/2M$ of the corresponding nucleus of mass M—i.e.,

$$S(q,\omega) = \frac{M}{q}J(y), \tag{5}$$

where y is the momentum $\mathbf{p}$ of the nucleus projected onto the scattering vector $\mathbf{q}$ (Refs. 25 and 26)—i.e., $y=\mathbf{p}\cdot\hat{\mathbf{q}}=(M/q)(\omega-\omega_r)=(M/q)(\omega-q^2/2M)$ where $\hat{\mathbf{q}}$ is the unit vector in the direction of the momentum transfer. $J(y)$ is the so-called Compton profile representing the momentum distribution of the scattering nucleus along y (Ref. 26). Thus, Eq. (4) can be rewritten in the following form:

$$C(\theta=\text{const},t_i) = Nb^2\frac{2}{L_0}\sqrt{\frac{2E_1}{m}}\Delta\Omega D(E_1)E_0(t_i)I(E_0(t_i))\frac{M}{q(t_i)}J(y(t_i)). \tag{6}$$

If atoms of different masses M are present in the sample, it follows, for the count rate in the time-of-flight channel t_i [Ref. 11, Eq. (2.22)], that

$$C(\theta=\text{const},t_i) = \sum_M C_M(t_i) = \left[\frac{E_0I(E_0)}{q}\right]_{t_i}\sum_M I_M M J_M(y_M(t_i)), \tag{7}$$

where

$$I_M = \frac{2}{L_0}D(E_1)\sqrt{\frac{2E_1}{m}}\Delta\Omega N_M b_M^2, \tag{8}$$

where N_M is the number of atoms of mass M and b_M is the bound scattering length for a given mass M. The set of brackets in Eq. (7) means that the value of $[E_0I(E_0)]/q$ is calculated pointwise for each time of flight t. The expression in the brackets is independent of the mass M of the scatterer and depends only on the parameters of the spectrometer and as such can be written in front of the sum over M. The West variable $y_M=y_M(t_i)$ is mass dependent as for each mass M there exists a different relation between time-of-flight value t_i and unique value of $y_M(t_i)$ corresponding to it with $y_M=0$ at the center of recoil peak for a given mass M. The momentum distributions $J_M(y_M)$ are assumed to have a normalized Gaussian form

$$J_M(y_M) = \frac{1}{\sqrt{2\pi\sigma_p(M)^2}}\exp\left(\frac{-y_M^2}{2\sigma_p(M)^2}\right), \tag{9}$$

with standard deviations $\sigma_p(M)$, which is also a common assumption in the NCS studies.[11,27–31]

In real experimental situations the measured count rate $C(\theta=\text{const},t_i)$ for every time of flight t_i is an average over the possible values of all geometrical parameters characterizing the paths of the neutrons L_0 and L_1 and the scattering angle θ as well as the final neutron energy E_1, weighed by their probability of occurrence. To account for this, a resolution function is introduced. (In what follows also the resolution function in the q-ω space is assumed to depend only on $q=|\mathbf{q}|$. For a more general account of the resolution function, see the Appendix.) The following approximation is made.[11] The distributions of the geometrical parameters are very well modeled by the Gaussian resolution functions R_t, R_{L_0}, R_{L_1}, and R_θ in the t, L_0, L_1, and θ spaces, respectively. The energy resolution function $R(E_1)$ in the E_1 space is also very well described by a Voigt function centered at 4.9 eV with a half width at half maximum (HWHM) of the Lorentzian part $\Delta_L=148$ meV and the standard deviation of the Gaussian part $\Delta_G=30$ meV. The transformation is made to express the original resolution functions R_t, R_{L_0}, R_{L_1}, R_θ, and R_{E_1} in the y

space for every mass M. The resolution functions in the y space are described by the same Gaussian or Voigt form. The widths of the resolution functions in y space are determined by multiplying their widths in the t, L_0, L_1, θ, and E_1 spaces with mass M-dependent Jacobians $|\partial y/\partial x_i|_M$ with $x_i=t$, L_0, L_1, θ, and E_1. The overall resolution function is calculated as a convolution of different resolution functions in the y space for a given mass M—i.e., $R_M(y_M)=R_{t,M}(y_M)\otimes R_{L_0,M}(y_M)\otimes R_{L_1,M}(y_M)\otimes R_{\theta,M}(y_M)\otimes R_{E_1,M}(y_M)$. The momentum distribution of the nuclei $J_M(y_M)$ [Eq. (9)] is convoluted with the mass-dependent resolution function $R_M(y_M)$. The resulting time-of-flight (TOF) spectrum $C(\theta=\text{const},t_i)$ can be written as

$$C(\theta=\text{const},t_i)=\left[\frac{E_0 I(E_0)}{q}\right]_{t_i}\sum_M I_M M J_M(y_M)\otimes R_M(y_M) \tag{10}$$

[Ref. 11, Eq. (2.24)].

In our experiments integrated peak intensities I_M are determined for every detector separately. I_M is proportional to the total bound scattering cross-section density $N_M\sigma_M$, where $\sigma_M=4\pi b_M^2$ is the total bound scattering cross section.[32] Hence, the measured value of $[I_H/I_X]_{expt}$ can be compared to the value of $[I_H/I_X]_{theor}=(N_H\sigma_H)/(N_X\sigma_X)$ calculated taking the tabulated[32] σ_M and the N_M known from chemical formula and/or sample preparation. The ratio

$$P=\frac{[I_H/I_X]_{expt}}{[I_H/I_X]_{theor}} \tag{11}$$

is smaller than unity in our experiments on hydrogen containing materials,[1–6] thus indicating the anomalous neutron Compton scattering from protons.

III. MODEL-FREE DATA REDUCTION SCHEME

Recently, an alternative NCS data reduction scheme has been proposed by Dorner.[22] It can be summarized in the following steps.

(1) The TOF spectrum $C(\theta,t_i)$ collected for a given fixed scattering angle θ is given by the convolution (in the q-ω space) of the dynamic structure factor $S(q(i),\omega(i))$ and the resolution function $R(q(i),\omega(i))$ [for the derivation see Eqs. (A1)–(A9) in the Appendix]:

$$C(\theta=\text{const},t_i)=\int R(\omega(t_i)+\Delta\omega,q(t_i)+\Delta q)\times S(\omega(t_i)+\Delta\omega,q(t_i)+\Delta q)\,d\Delta q\,d\Delta\omega. \tag{12}$$

$C(\theta,t_i)$ is normalized, dividing it pointwise (for each time of flight t_i) by the value of the phase-space volume for the incoming neutrons $V_0(t_i)$ [see Eqs. (14) and (A17) in the Appendix]. As a result, the quantity $C_{norm}(\theta,t_i)$ is obtained [see Eq. (A18) in the Appendix].

(2) The individual values of the TOF in $C_{norm}(\theta,t_i)$ are replaced by the corresponding values of the energy transfer $\omega(t_i)$. The values of $\omega(t_i)$ are calculated from t_i on the basis of the known geometrical parameters defining the neutron flight paths L_0, L_1, and θ and the value of E_1 from basic kinematic equations [see Ref. 11, Eqs. (2.3)–(2.7)]. It is worth noting that this replacement is done without any Jacobian. The spectrum $C_{norm}(\theta=\text{const},\omega(t_i))$ obtained in this way represents a constant-θ scan performed by the inverse-geometry TOF spectrometer in the q-ω space and contains peaks representing scattering from different masses present in the sample of interest.

(3) $C_{norm}(\theta=\text{const},\omega(t_i))$ is transformed into $C_{norm}(q=\text{const},\omega(t_i))$. At this point it is crucial to have well-separated peaks corresponding to the scattering from different masses M. After identifying the peaks each of $C_{norm,M}(\theta=\text{const},\omega(t_i))$ must be multiplied pointwise by the corresponding mass-dependent Jacobian for the transformation from the constant-θ scan into a fictitious constant-q scan. For deep inelastic scattering from atoms of mass M the Jacobian for an inverse time-of-flight instrument is [Ref. 21, Eq. (9)]

$$J=1-\frac{m}{M}\left(1-\frac{k_1}{k_0}\cos(\theta)\right), \tag{13}$$

being particularly simple for the case $m=M$ of hydrogen—i.e., $J=k_1/k_0\cos(\theta)$.

(4) The signals $C_{norm,M}(\omega(t_i),q=\text{const})$ are integrated over the respective ω range to obtain the scattering intensities from different masses M.

In the Appendix the details are described of the derivation of the resolution function and the count rate in the q-ω space [Eqs. (A1)–(A9)] as well as the phase volume V_0 [Eqs. (A10)–(A17)]. Here, we concentrate on few remarks concerning the steps (1), (3), and (4) of the above data reduction scheme that are in order.

Step (1). To normalize the instrument resolution function the count rate $C(t_i)$ has to be divided pointwise by the corresponding values of $V_0(t_i)$ [see Eq. (A19) in the Appendix]. The original derivation of the V_0 (Ref. 22) was for the incident neutron spectrum of the form $1/E_0$. In case of the VESUVIO spectrometer at ISIS the spectrum has the form $1/[E_0]^{0.9}$. The volume V_0 is given by [see the Appendix, Eq. (A17)]

$$V_0\sim\frac{E_0}{E_0^{0.9}}\Delta\Omega\Delta t_0, \tag{14}$$

where $\Delta\Omega$ is the constant angular acceptance of a detector and Δt_0 is the constant time bin in the data acquisition electronics. It is worth mentioning that $V_0\approx E_0 I(E_0)$, so the normalization of the count rate involves the division by $E_0 I(E_0)$.

Interestingly, the whole normalization to the constant incident neutron flux proposed by Dorner can be also found by Cowley.[21] Cowley also aims at obtaining $S(q,\omega)$ for a constant-q scan from the observed TOF spectra. The obtained $S(q=\text{const},\omega)$ can then be easily compared with theoretical predictions [e.g., in terms of the sum rules for $S(q,\omega)$]. He derives the two factors the TOF data points should be multiplied by when comparing the experimental scattering intensities with theoretical values. The first factor

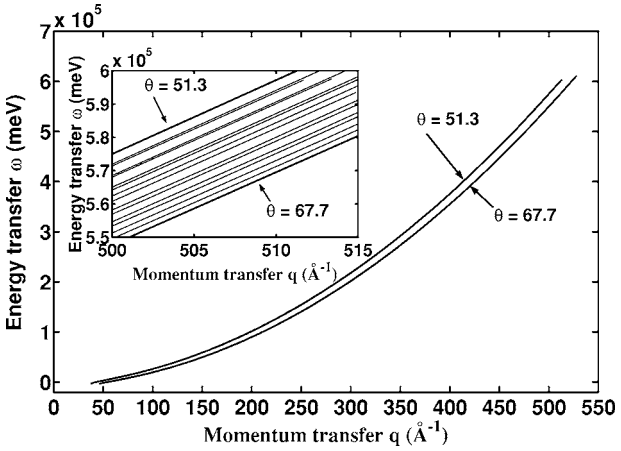

FIG. 2. Constant-θ scans at VESUVIO for forward scattering of neutrons from the polyethylene sample chosen for the comparison of the conventional NCS and the model-free data reduction schemes (see Sec. IV). For the picture clarity shown are the uppermost and lowermost trajectories only for θ=51.3° and θ=67.7°, respectively. Inset: the constant-θ scans for all 16 chosen forward detectors in the high-momentum transfer range. The scans are ordered from the smallest (θ=51.3°, the uppermost trajectory), to the biggest scattering angle (θ=67.7°, the lowermost trajectory).

$1/I(E_0)k_0^2$ is to account for the variation of the incident neutron flux with the incident neutron energy E_0. This factor is proportional to $1/V_0$ by Dorner.[22]

Step (3). For a typical measurement on Vesuvio consisting of 32 TOF spectra recorded for 32 different scattering angles θ in the range 35°–68° for forward scattering one gets a collection of "banana-shaped" curvilinear trajectories lying close to one another in the q-ω space.[33] There are two reasons why the constant-q scans cannot be extracted from a group of data collected for all forward detectors on VESUVIO and the above Jacobian must be used instead. First, the different detectors are not calibrated to collect the same absolute intensity of spectra. Thus the signals at the same values of q from different spectra at different scattering angles cannot be directly compared. Second, the range of ω values corresponding to the same q value for different detectors is too small to reconstruct the spectrum corresponding to a constant-q scan (see Fig. 2).

Thus, after identifying the signals $C_{norm,M}(\omega(i))$ corresponding to different masses M each of them must be multiplied pointwise by the corresponding mass-dependent Jacobian [see Eq. (13)]. At this point, the correction of the initial TOF data in the Dorner procedure is identical to the second correction proposed by Cowley.[21]

Step (4). In the last step of the analysis the signals $C_{norm,M}(\omega(t_i), q=\text{const})$ have to be integrated over ω to obtain the scattering intensities from different masses M. In the light of the experimental results (see below), showing that the convolution approximation and the approach by Dorner lead to the same "anomalies" of the scattering intensities from protons, it is especially interesting to also prove the equivalence of both schemes theoretically. Starting from Eq. (10) one can rewrite it in the following way:

$$C(\theta=\text{const},t_i) = E_0(t_i)I(E_0(t_i))\sum_M I_M \frac{M}{q(t_i)} J_M(y_M) \otimes R_M(y_M). \tag{15}$$

Knowing that

$$\frac{M}{q(t_i)} J_M(y_M) = S_M(q(t_i),\omega(t_i)) \tag{16}$$

and that the resolution function $R_M(y_M)$ can be written as $R_M(q(t_i),\omega(t_i))$, Eq. (15) can be written in the following way:

$$C(\theta=\text{const},t_i) = E_0(t_i)I(E_0(t_i))\sum_M I_M S_M(q(t_i),\omega(t_i)) \otimes R_M(q(t_i),\omega(t_i)), \tag{17}$$

where $\otimes$ means a two-dimensional convolution over the variables q and ω. The normalization [the pointwise division by $E_0(t_i)I(E_0(t_i)) \sim V_0(t_i)$] gives

$$C_{norm}(\theta=\text{const},t_i) = \sum_M I_M S_M(q(t_i),\omega(t_i)) \otimes R_{M,norm}(q(t_i),\omega(t_i)), \tag{18}$$

where

$$R_{M,norm}(q(t_i),\omega(t_i)) = R_M(q(t_i),\omega(t_i))/[E_0(t_i)I(E_0(t_i))] \sim R_M(q(t_i),\omega(t_i))/V_0(t_i) \tag{19}$$

is the normalized instrument resolution function for a given mass M as defined in the Appendix [Eq. (A19)]. This function is in turn proportional to the resolution function given by Dorner[22] with the proportionality constant $1/V_1$. This constant factor will cancel out in the ratio P given by Eq. (11) which is of main interest here. With the further assumption that one is able to separate the signals from individual masses one can write

$$C_{norm}(\omega(t_i), q=\text{const}) = \sum_M C_{norm,M}(\omega(t_i), q=\text{const}) = \sum_M C_{norm,M}(\omega(t_i), \theta=\text{const}) Jac_M(t_i), \tag{20}$$

where Jac_M is the Cowley's Jacobian given by Eq. (13) calculated pointwise for each mass M individually. Then one can write for each individual mass M replacing simply each value of the time of flight t_i with the corresponding value of $\omega(t_i)$:

$$C_{norm,M}(\omega(t_i), q=\text{const}) = I_M S_M(q=\text{const},\omega(t_i)) \otimes R_{M,norm}(q=\text{const},\omega(t_i)), \tag{21}$$

where $\otimes$ means a single convolution over the ω variable. Then, integrating over ω and using the properties of the convolution with the normalized resolution function and the sum rule for each mass M,

$$\int S_M(q=\text{const},\omega(t_i)) \otimes R_{M,norm}(q=\text{const},\omega(t_i))d\omega$$

$$= \int S_M(q=\text{const},\omega(t_i))d\omega = 1, \quad (22)$$

we finally obtain

$$\sum_M \int C_{norm,M}(\omega(t_i),q=\text{const})d\omega = \sum_M I_M = \sum_M N_M b_M^2. \quad (23)$$

The above equation shows the equivalence of the integrated constant-q scan in the q-ω space and the scattering intensity from the mass M obtained as a fitting parameter from the convolution approximation. Thus, the NCS data reduction scheme as used at ISIS and that proposed by Dorner are equivalent in that they lead to the same integrated scattering intensities.

IV. RESULTS

A polyethylene sample was chosen for the comparison of the conventional NCS and the model-free data reduction schemes. Low-density polyethylene foil (0.15 mm thick) was used directly for the neutron experiment.[34] The sample was hanging freely in the neutron beam. The standard neutron fitting procedure using the CA approximation[11] was performed. First, both widths of the momentum distribution $\sigma_p(H)$ and $\sigma_p(C)$ for H and D, respectively, and the scattering cross section densities I_H and I_C from hydrogen and carbon, respectively, were set as free fitting parameters for each forward spectrum (see Fig. 11 in Ref. 34). Then the average values of $\sigma_p(H)$ and $\sigma_p(C)$ over all scattering angles were found: $\sigma_p(\text{H})=4.6\pm0.1$ Å^{-1} and $\sigma_p(\text{C})=16.4\pm0.1$ Å^{-1}, respectively.[34] Very similar widths were observed in an earlier neutron Compton study of polyethylene.[35] Using the fixed values of $\sigma_p(\text{H})=4.6$ Å^{-1} and $\sigma_p(\text{C})=16.4$ Å^{-1}, the scattering cross-section densities I_H and I_C from hydrogen and carbon, respectively, were fitted once again for different forward-scattering angles using Eq. (10). The comparison of the obtained values of the scattering cross sections with the tabulated ones revealed the anomaly of the n-p cross section of about 50% for the scattering angles 53°–68° (Ref. 34).

The total number of 32 forward detector spectra are available at VESUVIO. However, for detectors placed at scattering angles smaller than ~50° the recoil peaks due to neutron scattering from protons overlap with the carbon recoil peaks. For the sake of comparison of the results of the analysis using the convolution approximation with the Dorner scheme one must choose the TOF spectra for which the recoil peaks do not overlap (for details see discussion in Sec. III). We have chosen TOF spectra for polyethylene measured by two forward detector banks, eight detectors each. The range of the scattering angles θ for the chosen detectors varied between 51.3° and 67.7°. In this angular range the TOF spectra consisted of two separated scattering peaks: one broad, intense peak centered at around 200 μs due to scattering on protons and a weaker carbon peak centered at around 370 μs. Thus, the chosen spectra fulfilled the criteria for the Dorner analysis.[22]

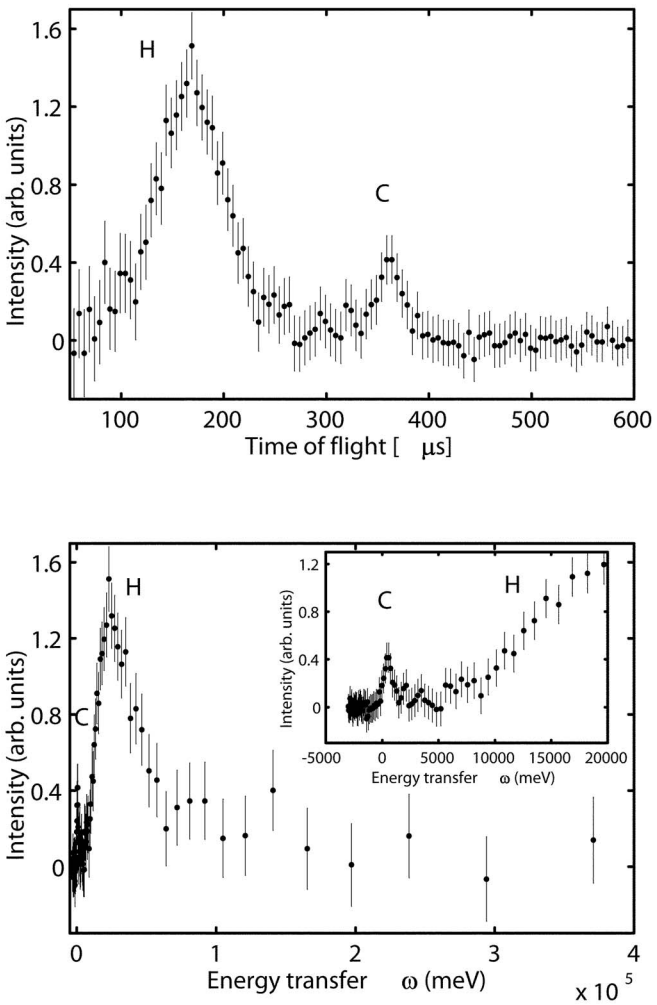

FIG. 3. NCS spectrum of polyethylene at the scattering angle $\theta=66.7°$. Top: the time-of-flight spectrum. Bottom: the spectrum transformed into the energy transfer variable ω and divided pointwise by $E_0(t_i)I(E_0(t_i))$.

An example of such spectrum for the detector at the scattering angle $\theta=66.7°$ is shown in Fig. 3. The spectrum was transformed to the energy transfer variable ω and normalized by dividing it pointwise by $E_0(t_i)I(E_0(t_i))$ to illustrate the first step of the analysis described above (Fig. 3, lower part).

The spectra $C_M(\theta=\text{const},\omega(t_i))$ corresponding to the scattering at $\theta=66.7°$ from the individual masses $M(1)=1$ and $M(2)=12$ amu, the Jacobians $Jac_M(t_i)$ of the transformation from a constant-θ scan into a constant-q scan, the factors $1/[E_0(t_i)I(E_0(t_i))]$, and the resulting normalized (multiplied pointwise by $Jac_M(t_i)/[E_0(t_i)I(E_0(t_i))]$) spectra $C_{norm,M}(q=\text{const},\omega(t_i))$ are shown in Figs. 4 and 5, respectively.

The position $t_M(L_0,L_1,\theta,E_1)$, in the time of flight, of a recoil-peak center for a given mass M is governed by the kinematics of the scattering process and is given by[11]

$$t = \frac{L_0}{v_0} + \frac{L_1}{v_1} \quad (24)$$

and

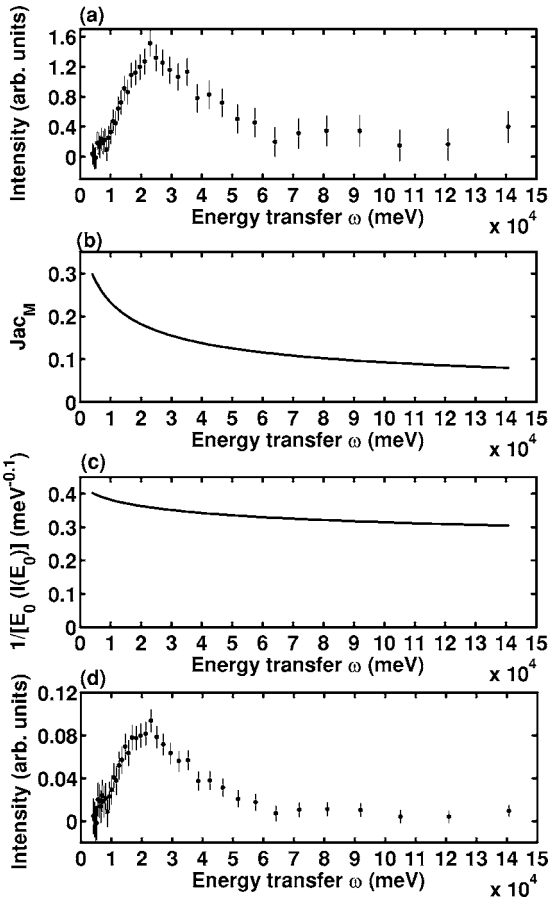

FIG. 4. The polyethylene sample. Detector at $\theta=66.7°$. Proton peak. (a) $C_M(\theta=\text{const},\omega(t_i))$, (b) Jacobian of the transformation from a constant-θ scan into a constant-q scan, (c) $1/[E_0(t_i)I(E_0(t_i))]$, and (d) $C_{norm,M}(\mathbf{q}=\text{const},\omega(t_i))=C_M(\theta,\omega(t_i))Jac_M(t_i)/[E_0(t_i)I(E_0(t_i))]$.

$$\frac{v_1}{v_0}=\frac{\cos(\theta)+\sqrt{(M/m)^2-\sin^2(\theta)}}{(M/m)+1}. \tag{25}$$

For different detectors their placement in the scattered neutron beam (determining the parameters L_0, L_1, and θ) is different. The absorber foil determines the final neutron energy E_1 and the final energy resolution $R_{E_1,M}(y_M)$. The above quantities are determined in a separate calibration measurement before each sample run on VESUVIO.[36] It is a straightforward conclusion from Eq. (25) that for heavier scatterer mass M, in the limit $M\gg m$, $v_1\cong v_0$, whereas for protons, where $M=m$, $v_1/v_0=\cos(\theta)$. Thus, in the angular range given above the proton peak will "move" slightly with scattering angle θ from detector to detector, whereas the position of the carbon peak remains practically constant. (For the carbon peak the integration limits are fixed between 325 μs and 425 μs—i.e., in the ω range between −1.05 eV and 1.87 eV. The variation of the above energy range from detector to detector, due to different values of L_0, L_1, and θ, is less than 0.02 eV.) The integration of the $S(q=\text{const},\omega)$ function for protons had to be performed over different energy transfer limits ω (see Table I) for different detectors.

The results of the complete analysis for the 16 detectors, as compared to the analysis previously performed on the polyethylene data[34] for the same detectors, are summarized in Fig. 6.

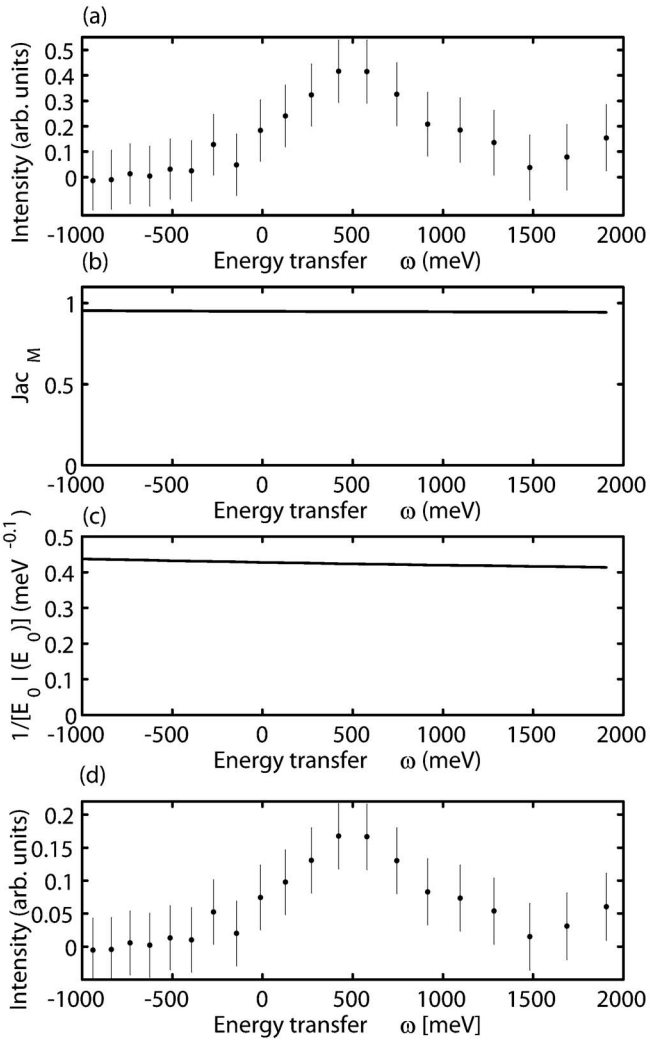

FIG. 5. The polyethylene sample. Detector at $\theta=66.7°$. Carbon peak. (a) $C_M(\theta=\text{const},\omega(t_i))$, (b) Jacobian of the transformation from a constant-θ scan into a constant-q scan, (c) $1/[E_0(t_i)I(E_0(t_i))]$, and (d) $C_{norm,M}(\mathbf{q}=\text{const},\omega(t_i))=C_M(\theta=\text{const},\omega(t_i))Jac_M(t_i)/[E_0(t_i)I(E_0(t_i))]$.

As can be seen from Fig. 6, both data treatment schemes yield the same results for the anomaly of the scattering cross section from protons within the statistical errors of both methods. The only discrepancy arising between the results of the CA and Dorner model-free reduction schemes arises for the smaller scattering angle range—i.e., between 51° and 54°. This is most probably due to some overlap between the H and C recoil peaks at these small angles. The lack of the total peak separation makes then the Dorner analysis inaccurate.

V. DISCUSSION

We have demonstrated theoretically the equivalence of the CA and model-free approach proposed by Dorner in the NCS data reduction as far as the scattering intensities are

TABLE I. The integration limits ω_H of $S(q=\text{const},\omega)$.

Detector	θ [deg]	L_0 [m]	L_1 [m]	TOF_H [μs]	ω_H [eV]
49	67.7	11.055	0.7051	85–305	2.85–137.5
50	65.7	11.055	0.7048	105–305	2.85–79.4
51	63.7	11.055	0.7048	105–305	2.85–79.4
52	61.7	11.055	0.7018	105–305	2.84–79.1
53	59.1	11.055	0.6971	105–305	2.83–78.7
54	57.5	11.055	0.6950	125–325	1.85–50.5
55	55.4	11.055	0.6930	125–325	1.85–50.4
56	53.2	11.055	0.6991	145–345	1.05–34.5
65	51.3	11.055	0.6932	155–355	0.7–28.9
66	53.6	11.055	0.6891	155–355	0.69–28.8
67	55.7	11.055	0.6898	125–325	1.85–50.3
68	58.0	11.055	0.6980	125–325	1.85–50.4
69	60.1	11.055	0.6851	105–305	2.81–78.2
70	62.4	11.055	0.6902	105–305	2.82–78.4
71	64.5	11.055	0.6913	105–305	2.82–78.5
72	66.7	11.055	0.7054	85–285	4.04–136.4

concerned [Eqs. (15)–(23)]. We have also shown that both data treatments lead to the same results for the anomaly of the scattering cross-section density ($N_M\sigma_M$) from protons in the polyethylene sample. We believe that this result provides direct and strong evidence against previous comments[12–14,20,21] concerning the NCS data reduction scheme using the CA as applied on VESUVIO.

Independently of the question of choosing the most accurate and transparent data reduction scheme, the issueemerges about the physical origin and mechanisms explaining the striking anomaly under consideration.

It was proposed[1–6] that the anomaly of the scattering cross section from protons is caused by short-lived entanglement, in which the quantum dynamics of protons and surrounding particles is connected. Such entanglement can exist at room temperature on the subfemtosecond time scale.[37] The entangled states would then decay to normal factorizable multiparticle states, thus recovering the conventional scattering intensities.[3,38–40] However, the time scale of the neutron Compton scattering event is short enough for the decoherence processes destroying the entanglement not to be fully effective.[1,3,40,41]

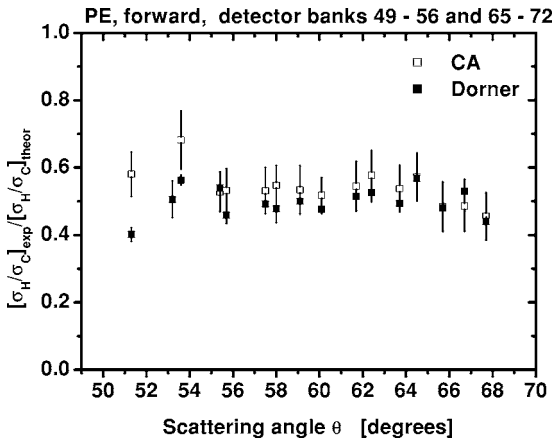

FIG. 6. Results of the data reduction on the polyethylene sample for all chosen 16 forward detectors. The results of the data analysis proposed (Ref. 22) are compared to the analysis previously performed using the CA. Open squares: the CA approximation. Solid squares: Dorner's method. It is shown that both methods yield the same results.

As the entanglement is believed to be governed by the short-time-scale dynamics, the issue of the breakdown of the Born-Oppenheimer approximation during the scattering process appears in theoretical models either in combination with short-time-scale entanglement[40] or in connection with electronic excitations[42,43] (see also related theoretical considerations, Refs. 44 and 45).

A different theoretical model stresses the importance of quantum exchange correlations in the observed effect[38,39,46] (see also related comments, Refs. 44 and 47).

Our present result demonstrates that no matter what the functional form of any resolution function including the energy resolution and the form of the momentum distribution, the scattering intensities obtained from the data analysis will be the same. This conclusion is of importance as it demonstrates the genuineness of the scattering cross-section anomaly from protons in the most transparent and straightforward manner. With this we hope that the mainstream discussion about the striking effect under consideration will focus from now on more on its most interesting aspect—namely, on the physical explanations mentioned above and/or additional ones.

ACKNOWLEDGMENT

Financial support form the EU in the framework of the QUACS RTN programme is acknowledged.

APPENDIX

This appendix aims at presenting, in a straightforward manner, the basic formulas for the time-of-flight data reduction scheme proposed by Dorner[22] and the formalism to describe the resolution function in the $\mathbf{q}$-ω space introduced by Komura and Cooper,[48] further developed by Todate *et al.*[49] and used by Dorner in his original derivation.[22] The formalisms mentioned above are adopted to the special case of the inverse-geometry TOF spectrometer VESUVIO at ISIS.

In what follows the energies of the incoming and scattered neutrons, E_0 and E_1, respectively, as well as the energy transfer variable ω are expressed in eV. The momenta of incoming and scattered neutrons, $\mathbf{k}_0$ and $\mathbf{k}_1$, respectively, as well as the momentum transfer variable $\mathbf{q}$, are expressed in Å^{-1}.

The starting point of Dorner's analysis is the double-differential cross section $d^2\sigma/d\Omega dE_1$ [Eq. (1), Ref. 22]. It describes the probability for an infinitesimal (calculated per phase-space volume) flux of incoming neutrons $dj(\mathbf{k}_0)(t_i)$ to be scattered into a solid angle $d\Omega$ after scattering into a window dE_1 of final energy.

The intensity $dC(\theta=\text{const},t_i)$ collected in a detector at a scattering angle θ is then [Eq. (2), Ref. 22]

$$dC(\theta=\text{const},t_i) = dj(\mathbf{k}_0(t_i))\frac{d^2\sigma}{d\Omega dE_1}d\Omega dE_1 p(\mathbf{k}_1), \quad \text{(A1)}$$

where $p(\mathbf{k}_1)$ contains characteristics of the spectrometer after the sample.

The flux of incoming neutrons $dj(\mathbf{k}_0)(t_i)$ is defined as [Eq. (3) Ref. 22]

$$dj(\mathbf{k}_0(t_i)) = p(\mathbf{k}_0(t_i))\mathbf{k}_0(t_i)dk_{0,x}dk_{0,y}dk_{0,z}, \quad \text{(A2)}$$

where $p(\mathbf{k}_0)(t_i)$ is the spectrum (per phase-space volume) of the incoming neutrons.

The double-differential cross section is related to the dynamic structure factor [see Eq. (1)] in the following way:

$$\frac{d^2\sigma}{d\Omega dE_1} = Nb^2\sqrt{\frac{E_1}{E_0}}S(\mathbf{q},\omega). \quad \text{(A3)}$$

We further choose our coordinate system in such a way that the z direction coincides with the direction of $\mathbf{k}_1$. We can then write $d\Omega = dk_{1,x}dk_{1,y}/k_1^2$ and $dE_1 \sim k_1 dk_1$. Then, using Eqs. (A1)–(A3) the intensity dC at the detector [Eq. (A1)] reads

$$dC(\theta=\text{const},t_i) = p(\mathbf{k}_0(t_i))d\mathbf{k}_0 Nb^2 S(\mathbf{q}(t_i),\omega(t_i))p(\mathbf{k}_1)d\mathbf{k}_1. \quad \text{(A4)}$$

The above equation describes an idealized situation. In such an ideal measurement for a given time-of-flight channel t_i there exists only one combination of $\mathbf{k}_0(t_i)$ and $\mathbf{k}_1(t_i)$ leading to one value of $\mathbf{q}(t_i)$ and $\omega(t_i)$ (one point in the $\mathbf{q}$-ω space). In reality, however, the instrument has a finite resolution. It means that there exist many combinations of $\mathbf{k}_0$ and $\mathbf{k}_1$ all contributing to the same value of $\mathbf{q}(t_i)$ and $\omega(t_i)$. For each such combination there exists a $\mathbf{q}=\mathbf{k}_1-\mathbf{k}_0$ and an $\omega = (\hbar^2/2m)(k_0^2-k_1^2)$. The value of the resolution function at a given point in the $\mathbf{q}$-ω space $R(\omega,\mathbf{q})$ is obtained by integrating the probability distribution of $\mathbf{q}$ and ω over all possible paths $(\mathbf{k}_0,\mathbf{k}_1)$ to that point[48]:

$$R(\omega,\mathbf{q}) = \int P(\omega,\mathbf{q})d\mathbf{k}_0 d\mathbf{k}_1. \quad \text{(A5)}$$

We define $\Delta\mathbf{k}_0=\mathbf{k}_0-\mathbf{k}_0(t_i)$ and $\Delta\mathbf{k}_1=\mathbf{k}_1-\mathbf{k}_1(t_i)$. Thus, $\Delta\mathbf{q}=\mathbf{q}-\mathbf{q}(t_i)=\Delta\mathbf{k}_1-\Delta\mathbf{k}_0$. Additionally, we define $\Delta\omega=\omega-\omega(t_i)$. The point $(\omega,\mathbf{q})$ is placed at a distance $(\Delta\mathbf{q},\Delta\omega)$ from $(\omega(t_i),\mathbf{q}(t_i))$. Thus, we can write $R(\omega,\mathbf{q})$ as

$$R(\omega(t_i)+\Delta\omega,\mathbf{q}(t_i)+\Delta\mathbf{q}) = \int P(\omega(t_i)+\Delta\omega,\mathbf{q}(t_i)+\Delta\mathbf{q})d\Delta\mathbf{k}_0 d\Delta\mathbf{k}_1. \quad \text{(A6)}$$

The six-dimensional set of variables $(\Delta\mathbf{k}_0,\Delta\mathbf{k}_1)$ can be expressed through a four-dimensional set $\Delta\mathbf{q}$, $\Delta\omega$ using the fact that the variables $(\Delta\mathbf{k}_0,\Delta\mathbf{k}_1)$ are not all linearly independent.[48] The components $\Delta k_{0,x}$, $\Delta k_{0,y}$, $\Delta k_{1,x}$, and $\Delta k_{1,y}$ can be expressed as linear combinations of the components Δq_x, Δq_y, and $\Delta\omega$. The difference of components $\Delta k_{1,z}$ and $\Delta k_{0,z}$ is equal to Δq_z. Now, the resolution function reads[48]

$$R(\omega(t_i)+\Delta\omega,\mathbf{q}(t_i)+\Delta\mathbf{q}) = \int P(\omega(t_i)+\Delta\omega,\mathbf{q}(t_i)+\Delta\mathbf{q})d\Delta\mathbf{q}d\Delta\omega. \quad \text{(A7)}$$

The above integration is performed over a four-dimensional volume $(\Delta q_x,\Delta q_y,\Delta q_z,\Delta\omega)$. Using a Gaussian approximation for the probability distribution $P(\omega(t_i)+\Delta\omega,\mathbf{q}(t_i)+\Delta\mathbf{q})$ one can derive an analytical formula for $R(\omega(t_i)+\Delta\omega,\mathbf{q}(t_i)+\Delta\mathbf{q})$ [Eq. (14), Ref. 48]:

$$R(\omega(t_i)+\Delta\omega,\mathbf{q}(t_i)+\Delta\mathbf{q}) = R(\omega(t_i),\mathbf{q}(t_i))\exp\left\{-\frac{1}{2}\sum_{k=1}^{4}\sum_{l=1}^{4}M_{kl}X_kX_l\right\}, \quad \text{(A8)}$$

with $X_1=\Delta q_x$, $X_2=\Delta q_y$, $X_3=\Delta q_z$, and $X_4=\Delta\omega$. For a constant value of probability one yields so-called probability ellipsoids in the four-dimensional space.[48,49]

The count rate $C(\theta=\text{const},t_i)$ in a time-of-flight channel t_i for a detector placed at a scattering angle θ is given by a convolution of the dynamic structure factor with the resolution function given by Eq. (A7):

$$C(\theta=\text{const},t_i) = \int R(\omega(t_i)+\Delta\omega,\mathbf{q}(t_i)+\Delta\mathbf{q}) \times S(\omega(t_i)+\Delta\omega,\mathbf{q}(t_i)+\Delta\mathbf{q})d\Delta q d\Delta\omega \quad \text{(A9)}$$

[see Eq. (16), Ref. 48].

To normalize the above count rate one has to divide Eq. (A9) by the integral, over the $\Delta\omega$-$\Delta\mathbf{q}$ space, from the resolution function. This integral is equal to the product of the volume elements V_0 and V_1 for the incident and scattered neutrons, respectively.[50] The volume elements are defined as[51]

$$V_0(t_i) = \int p(\mathbf{k}_0(t_i))d\mathbf{k}_0 \tag{A10}$$

and

$$V_1 = \int p(\mathbf{k}_1)d\mathbf{k}_1. \tag{A11}$$

As the volume element V_1 is constant in the inverse time-of-flight spectrometer, the same value of V_1 would appear in the normalized count rate $C_{norm}(\theta=\text{const},t_i) = C(\theta=\text{const},t_i)/[V_0V_1]$ for each value of the time of flight t_i and, consequently, for each mass M the neutron is scattered from. Thus, during the normalization of the resolution function it is sufficient to divide the count rate $C(\theta=\text{const},t_i)$ only by $V_0(t_i)$.

In what follows, the quantities $C_{norm}(\theta=\text{const},t_i)$ and $R_{norm}(\omega(t_i),\mathbf{q}(t_i))$ will be defined as $C(\theta=\text{const},t_i)/V_0(t_i)$ and $R(\omega(t_i),\mathbf{q}(t_i))/V_0(t_i)$, respectively. The original derivation of the V_0 was done by Dorner[22] for the incident neutron spectrum of the form $1/E_0$. To find the expression for V_0 in case of the VESUVIO spectrometer we start with the expression for the flux f of epithermal neutrons per solid angle $d\Omega$ and initial neutron energy dE_0. In the case of neutrons leaving the moderator at ISIS spallation source,

$$f(E_0(t_i)) = \frac{1}{E_0(t_i)^{0.9}}d\Omega_0 dE_0. \tag{A12}$$

Bearing in mind that $dE_0 \sim k_0 dk_0$ we can further write

$$f(k_0(t_i)) = \frac{1}{k_0(t_i)^{0.8}}d\Omega_0 dk_0. \tag{A13}$$

Thus, the distribution of incoming neutrons $n(k_0(t_i))$ per solid angle $d\Omega$ and initial neutron energy dE_0 reads

$$n(k_0(t_i)) = \frac{1}{k_0(t_i)^{1.8}}d\Omega_0 dk_0. \tag{A14}$$

Setting $k_0(t_i)^2 d\Omega_0 = dk_{0,x}dk_{0,y}$ and $dk_0 \equiv dk_{0,z}$ one can derive the distribution $n(k_0(t_i))$ per volume $V_0(t_i)$:

$$n(k_0(t_i)) = \frac{1}{k_0(t_i)^{3.8}}dk_{0,x}dk_{0,y}dk_{0,z} = p(k_0(t_i))dk_{0,x}dk_{0,y}dk_{0,z}, \tag{A15}$$

with $p(k_0(t_i)) = 1/[k_0(t_i)^{3.8}]$. Finally, the volume V_0 is given by Eq. (A10):

$$V_0(t_i) = \int \frac{1}{k_0(t_i)^{3.8}}dk_{0,x}dk_{0,y}dk_{0,z}. \tag{A16}$$

Using the relation $k_0(t_i)^2 dk_0 d\Omega_0 = dk_{0,x}dk_{0,y}dk_{0,z}$ and $k_0(t_i) \sim 1/t_i$, we get $dk_{0,x}dk_{0,y}dk_{0,z} \sim d\Omega dt/t_i^4$, and the volume element $V_0(t_i)$ yields[22]

$$V_0(t_i) \sim \int_0^{\Delta\Omega_0,\Delta t_0} \frac{1}{k_0(t_i)^{3.8}}\frac{d\Omega dt}{t_i^4} \sim \frac{k_0(t_i)^4}{k_0(t_i)^{3.8}}\Delta\Omega_0\Delta t_0 \sim \frac{E_0(t_i)}{E_0(t_i)^{0.9}}\Delta\Omega_0\Delta t_0, \tag{A17}$$

where $\Delta\Omega$ is the constant angular acceptance of a detector and Δt_0 is the constant time bin in the data acquisition electronics.

Using the Eq. (A17) one can express the normalized count rate at a constant scattering angle $C_{norm}(\theta=\text{const},t_i)$ as

$$C_{norm}(\theta=\text{const},t_i) \sim \int R(\omega(t_i)+\Delta\omega,\mathbf{q}(t_i)+\Delta\mathbf{q})S(\omega(t_i)+\Delta\omega,\mathbf{q}(t_i)+\Delta\mathbf{q})d\Delta\mathbf{q}d\Delta\omega \Big/ \left[\frac{E_0(t_i)}{E_0(t_i)^{0.9}}\right]. \tag{A18}$$

and the normalized resolution function as

$$R_{norm}(\omega(t_i)+\Delta\omega,\mathbf{q}(t_i)+\Delta\mathbf{q}) \sim \int P(\omega(t_i)+\Delta\omega,\mathbf{q}(t_i)+\Delta\mathbf{q})d\Delta\mathbf{q}d\Delta\omega \Big/ \left[\frac{E_0(t_i)}{E_0(t_i)^{0.9}}\right]. \tag{A19}$$

*Electronic address: krzystyniak@iwan.chem.tu-berlin.de

[1] C. A. Chatzidimitriou-Dreismann, T. Abdul-Redah, R. M. F. Streffer, and J. Mayers, Phys. Rev. Lett. **79**, 2839 (1997).
[2] T. Abdul-Redah and C. A. Chatzidimitriou-Dreismann, Physica B **350**, e1035 (2004).
[3] C. A. Chatzidimitriou-Dreismann, T. Abdul Redah, and J. Sperling, J. Chem. Phys. **113**, 2784 (2000).
[4] C. A. Chatzidimitriou-Dreismann, T. Abdul Redah, R. M. F. Streffer, and J. Mayers, J. Chem. Phys. **116**, 1511 (2002).
[5] C. A. Chatzidimitriou-Dreismann, T. Abdul Redah, and B. Kolaric, J. Am. Chem. Soc. **123**, 11945 (2001).
[6] E. B. Karlsson, T. Abdul-Redah, R. M. F. Streffer, B. Hjörvarsson, J. Mayers, and C. A. Chatzidimitriou-Dreismann, Phys. Rev. B **67**, 184108 (2003).
[7] C. A. Chatzidimitriou-Dreismann, M. Vos, C. Kleiner, and T. Abdul-Redah, Phys. Rev. Lett. **91**, 057403 (2003).

[8] Phys. Today Physics Update, **56**(9), 9 (2003).
[9] J. R. Minkel, Sci. Am. (Int. Ed.) **289**(4), 20 (2003).
[10] P. Schewe, J. Riordon, and B. Stein, *The AIP Bulletin of Physics News, Physics News Update*, No. 648 (AIP, Melville, NY, 2003).
[11] J. Mayers and T. Abdul-Redah, J. Phys.: Condens. Matter **16**, 4811 (2004).
[12] J. J. Blostein, J. Dawidowski, and J. R. Granada, Physica B **304**, 357 (2001).
[13] J. J. Blostein, J. Dawidowski, and J. R. Granada, Physica B **334**, 257 (2003).
[14] J. J. Blostein, J. Dawidowski, and J. R. Granada, Phys. Rev. B **71**, 054105 (2005).
[15] P. F. Rose and C. L. Dunford, Nuclear Data File ENDF-6; see www.nndc.bnl.gov
[16] C. A. Chatzidimitriou-Dreismann, T. Abdul-Redah, and J. Mayers, Physica B **315**, 281 (2002).
[17] P. A. Seeger, A. D. Taylor, and R. M. Brugger, Nucl. Instrum. Methods Phys. Res. A **240**, 98 (1985).
[18] T. Abdul-Redah, M. Krzystyniak, and C. A. Chatzidimitriou-Dreismann, Phys. Rev. B **72**, 052202 (2005).
[19] R. Senesi, D. Colognesi, A. Pietropaolo, and T. Abdul-Redah, Phys. Rev. B **72**, 054119 (2005).
[20] J. J. Blostein, J. Dawidowski, and J. R. Granada, Nucl. Instrum. Methods Phys. Res. B **217**, 333 (2004).
[21] R. A. Cowley, J. Phys.: Condens. Matter **15**, 4143 (2003).
[22] B. Dorner, J. Neutron Res. (to be published).
[23] L. van Hove, Phys. Rev. **95**, 249 (1954).
[24] G. L. Squires, *Introduction to the Theory of Thermal Neutron Scattering* (Dover, Mineola, NY, 1996).
[25] V. F. Sears, Phys. Rev. B **30**, 44 (1984).
[26] G. I. Watson, J. Phys.: Condens. Matter **8**, 5955 (1996).
[27] J. Mayers, C. Andreani, and G. Baciocco, Phys. Rev. B **39**, 2022 (1989).
[28] J. Mayers, Phys. Rev. B **41**, 41 (1990).
[29] J. Mayers, Phys. Rev. Lett. **71**, 1553 (1993).
[30] C. Andreani, D. Colognesi, and E. Pace, Phys. Rev. B **60**, 10008 (1999).
[31] A. C. Evans, D. N. Timms, J. Mayers, and S. M. Bennington, Phys. Rev. B **53**, 3023 (1996).
[32] S. W. Lovesey, *Theory of Neutron Scattering from Condensed Matter* (Clarendon, Oxford, 1984).
[33] J. Mayers and A. C. Evans, Rutherford Appleton Laboratory Report No. RAL 91 048, 1991 (unpublished).
[34] M. Vos, C. A. Chatzidimitriou-Dreismann, T. Abdul-Redah, and J. Mayers, Nucl. Instrum. Methods Phys. Res. B **227**, 233 (2005).
[35] B. Gabrys, W. Zajac, J. Mayers, and M. Kalhoro, Appl. Phys. A: Mater. Sci. Process. **74**, (Suppl.), S1645 (2002).
[36] A. L. Fielding and J. Mayers, Nucl. Instrum. Methods Phys. Res. A **480**, 680 (2002).
[37] C. A. Chatzidimitriou-Dreismann, Adv. Chem. Phys. **99**, 393 (1997).
[38] E. B. Karlsson and S. W. Lovesey, Phys. Rev. A **61**, 062714 (2000).
[39] E. B. Karlsson and S. W. Lovesey, Phys. Scr. **65**, 112 (2002).
[40] C. A. Chatzidimitriou-Dreismann, Laser Phys. **15**, 780 (2005).
[41] C. A. Chatzidimitriou-Dreismann, J. Alloys Compd. **356–357**, 244 (2003).
[42] G. F. Reiter and P. M. Platzman, Phys. Rev. B **71**, 054107 (2005).
[43] N. I. Gidopoulos, Phys. Rev. B **71**, 054106 (2005).
[44] D. Colognesi, Physica B **344**, 73 (2004).
[45] D. Colognesi, Physica B **358**, 114 (2005).
[46] E. B. Karlsson, Phys. Rev. Lett. **90**, 095301 (2003).
[47] H. Sugimoto, H. Yuuki, and A. Okumura, Phys. Rev. Lett. **94**, 165506 (2005).
[48] S. Komura and M. J. Cooper, Jpn. J. Appl. Phys. **9**, 866 (1970).
[49] Y. Todate, S. Taniguchi, and K. Tajima, Jpn. J. Appl. Phys., Part 2 **36**, L1474 (1997).
[50] B. Dorner, Acta Crystallogr., Sect. A: Cryst. Phys., Diffr., Theor. Gen. Crystallogr. **28**, 319 (1972).
[51] H. Maier-Leibnitz, Nukleonik **8**, 61 (1966).